

## SIMULATION OF NEURAL NETWORKS TO SENSORLESS CONTROL OF SWITCHED RELUCTANCE MOTOR

H S Ooi and T C Green

Imperial College, UK

Abstract - Neural networks have been applied to two aspects of sensorless switched reluctance motor operation. First a neural network is trained to predict position from inductance and phase current data and thereby eliminate the position sensor. Second, a neural network is trained to provide a current reference that minimises torque ripple. Torque ripple minimisation is achieved without a torque sensor. A model built in Matlab is used to simulate the system and show successful operation provided the training data is well chosen.

### I. INTRODUCTION

The switched Reluctance Motor(SRM) has now become a promising candidate for various general purpose adjustable speed applications because of its simplicity and robustness.

The SRM is controlled by switching the phase currents in synchronism with the regions of rising inductance of the stator windings of the motor. As the rotor pole moves from being unaligned to the aligned with a stator pole, the inductance of that stator coil varies from a minimum value to a maximum value. A rotor position sensor is used for detecting the angular position of the rotor and the region of inductance increase, and therefore of current commutation inferred. The position sensor is a significant contribution to the cost and complexity, and tend to reduced the reliability of the drive system.

Besides the drawback of using the position sensor, SRM is also renowned for its high torque ripple characteristic. The origin of the torque ripple in an SRM is the highly non-linear and discrete nature of the torque production mechanism. The torque ripple is significant at the commutation instant. The total torque in an SRM is the sum of torque generated by each of the stator phases which are controlled independently.

The SRM produces torque on the basis of varying reluctance along the magnetic circuit. When a stator phase is energised, the stator pole pair attracts the closest rotor pole pair toward alignment of the poles. Torque is produced by this tendency of the magnetic circuit to adopt a minimum reluctance configuration and is independent of the direction of the current flow. By

consecutive energization of successive phases, continuous rotation in either direction is possible.

The model of the SRM used in the simulation was based on a trigonometric function for the variation of the unsaturated inductance with the rotor position and a hyperbolic function for saturation approximation. The production of the torque was calculated based on the rate of change of the co-energy with the rotation angle. The equations used to obtain a model of the behaviour of SRM are:

(i) Cosine approximation of unsaturated inductance variation with rotor position

$$L_{unsat}(\theta) = L_{min} + (L_{max} - L_{min}) \left( \frac{1}{2} (1 - \cos(\theta \cdot N_{rotor\_pole})) \right) \quad (1)$$

(ii) Saturation approximation for inductance function

$$L(i, \theta) = L_{sat} + (L_{unsat}(\theta) - L_{sat}) \left( \operatorname{sech} \left( \frac{L_{unsat}(\theta) - L_{sat}}{\psi_{sat}(\theta)} \cdot i \right) \right)^2 \quad (2)$$

(iii) Saturation approximation for flux-linkage function

$$\psi(i, \theta) = L_{sat} \cdot i + \psi_{sat}(\theta) \cdot \tanh \left( \frac{L_{unsat}(\theta) - L_{sat}}{\psi_{sat}(\theta)} \cdot i \right) \quad (3)$$

where  $\theta$  is the rotor position  
 $i$  is the phase current  
 $N_{rotor\_pole}$  is number of rotor poles  
 $L_{min}$  is the unsaturated inductance in unaligned position  
 $L_{max}$  is the unsaturated inductance in aligned position  
 $L_{sat}$  is the saturated value of a winding inductance

The inductance generated by a single stator phase winding for various constant currents is plotted as shown in Figure 1.

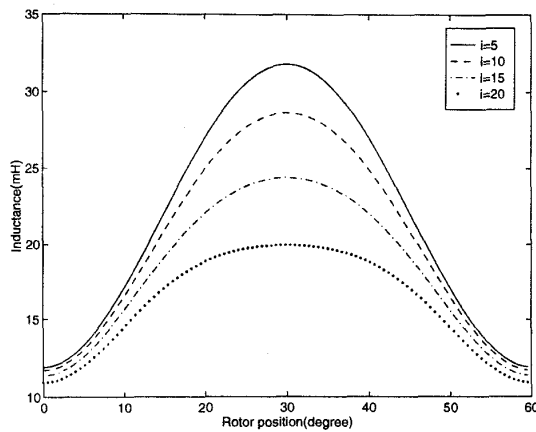


Figure 1: Graph of inductance versus rotor position

## II. REVIEW OF PREVIOUS METHODS

### 1. Position Sensorless Operation

The alternative to a position sensor is indirect rotor position sensing based on the measurement of motor parameters. These techniques can be classified into two board categories :

- (i) Non-intrusive methods where position information is obtained from terminal measurements of voltages and currents and the associated computations
- (ii) Active probing methods where low level high-frequency signals are injected into an idle phase to determine the position dependent inductance characteristic.

### 2. Torque Ripple Minimisation

Various torque ripple minimisation methods have been proposed which can be categorised into two main sections:

- (i) Neural network based approach described by Reay et al (1) and O'Donovan et al (2) where the neural network is used to approximate the inverse of the non-linear torque-angle-current characteristic or flux-linkage characteristic. The desired phase currents for minimum torque ripple production were obtained from the trained neural network on-line and off-line respectively
- (ii) Phase current optimising approach described by Schramm et al (3) and Hussain and Ehsani (4) for smooth torque production is achieved by analytically optimising the profile of the phase currents.

The torque ripple minimisation techniques described above required the use of a rotor position sensor and also a measurement of torque in Reay et al (1) and Hussain and Ehsani (3).

## III. PROPOSED SENSORLESS OPERATION

Three multi-layer feedforward neural networks are used to approximate the non-linear functions of  $\theta=f(L,i)$ ,  $\psi=g(i,\theta)$  and  $i=h(T,\theta)$  where  $\theta$ ,  $L$ ,  $i$ ,  $T$ ,  $\psi$  are rotor position, phase inductance, phase current, torque/phase and flux-linkage/phase respectively.

### 1. Rotor Position Estimation

A two-hidden-layer neural network with five neurons on each hidden layer is used to estimate the angular position  $\theta$  of a 4-phase SRM. The inductance,  $L$  of each the stator phase is a function of the supplied current  $i$  and of the angular position  $\theta$ . In order to determine the angular position  $\theta$ , the neural network is used to approximate the inverse of the function, i.e. to approximate the mapping of  $\theta=f(L,i)$ . Since the angular position  $\theta$  is dependent on the value of the current and inductance of each phase, these parameters, i.e.  $i_1, i_2, i_3, i_4$  and  $L_1, L_2, L_3, L_4$  have been chosen as the inputs of the neural networks. The angular period of the motor behaviour is defined by the number of rotor poles. In this simulation, a 8/6 SRM was modelled and therefore the angular period is  $60^\circ$ . The neural networks was therefore trained to approximate the rotor position within the interval  $0^\circ$ - $60^\circ$ . The neural network is trained off-line to estimate the sine and cosine of rotor position  $\theta$  to eliminate any discontinuities that can occur if the rotor position of  $0^\circ$ - $60^\circ$  were to be estimated directly. The Levenberg Marquardt training algorithm was used.

### 2. Torque Ripple Minimisation

A single hidden layer neural network with five hidden neurons is used to estimate the phase flux-linkage  $\psi$  of the 4-phase SRM. Since the flux-linkage  $\psi$  is dependent of the phase current  $i$  and also the rotor position  $\theta$ , the neural network is trained with these parameters to estimate the phase flux-linkage  $\psi$  function i.e.  $\psi=g(i,\theta)$ . Once the neural network is trained, it can be used to estimate the flux-linkage  $\psi_n$  of the other phases with the respective phase current  $i_n$  and rotor position  $\theta_n$  of that phase. As shown by O'Donovan et al (2), the parameters of the trained flux-linkage neural network can be used to estimate the torque/phase  $T$ . The estimated torque/phase  $\hat{T}_n$  for each phase of the SRM can be summed to estimate the overall torque  $\hat{T}$  generated by the SRM. The activation function of the hidden layer and the output layer of this neural network have to be a hyper-tangent sigmoid and linear functions respectively in

order for the torque/phase  $T$  to be evaluated algebraically.

In order to evaluate torque from flux-linkage for any phase of the SRM motor, it is necessary to determine the field co-energy,  $\omega'$  from the flux-linkage/phase,  $\psi$ . The field co-energy,  $\omega'$  is differentiated with respect to the rotor position,  $\theta$  to obtain the expression of the electromagnetic torque/phase,  $T$

$$\omega_n = \int_0^i \psi_n di_n \quad (4)$$

$$T_n(i_n, \theta) = \frac{\partial \omega_n}{\partial \theta} \quad (5)$$

where  $n$  is the  $n$ th phase of the motor.

The mathematical expression of the flux-linkage  $\psi$  neural network can be expressed as

$$\hat{\psi} = B_o + \sum_{j=1}^N W_j \text{Tanh}(\theta W_{j\theta} + i W_{ji} + B_j) \quad (6)$$

where  $B_o$  is the bias at the output layer  
 $W_j$  is the weights at the output layer  
 $B_j$  is the bias at the output layer  
 $W_{j\theta}$  is the weights at the hidden layer connecting the rotor position input  $\theta$   
 $W_{ji}$  is the weights at the hidden layer connecting the current input  $I$   
 $N$  is the number of hidden neurons

By substituting equation (6) into (4) and (5), the estimated torque can be computed algebraically as

$$\hat{T} = \sum_{j=1}^N W_j \frac{W_{j\theta}}{W_{ji}} \text{Tanh}(\theta W_{j\theta} + i W_{ji} + B_j) - \sum_{j=1}^N W_j \frac{W_{j\theta}}{W_{ji}} \text{Tanh}(\theta W_{j\theta} + B_j) \quad (7)$$

This shows that torque/phase  $T$  can be estimated from the parameters of the flux-linkage approximation neural network after it is well trained.

The Levenberg Marquardt algorithm which has been shown to have a fast convergence in function approximation is used for the training of the neural network off-line.

A third neural network with two hidden layers of seven neurons on each hidden layer is chosen to approximate the non-linear function of  $i=h(T, \theta)$  in order to generate current reference commands for a given torque. The estimated torque/phase  $\hat{T}_n$  computed from the flux-linkage approximation neural network parameters is used as the training input. The training of this neural network was accomplished off-line using the Levenberg Marquardt algorithm.

In the approach to minimise torque ripple of a SRM, there are three neural networks which were well trained to approximate the non-linear function of  $\theta=f(L, i)$ ,  $\psi=g(i, \theta)$  and  $i=h(\hat{T}, \theta)$  respectively. This will introduce a sensorless control of the SRM without the need of rotor position sensor and the measurement of torque production. The torque ripple minimisation method is based on generating a torque contour waveform using the trigonometry function during the overlapping period of the torque production for each phase of the SRM. For a 8/6 SRM, a typical torque contour waveform which is suitable for this purpose is

$$f(\theta) = 0.5 + 0.5 \sin(4.N\_rotor\_pole.\theta) \quad (8)$$

where  $N\_rotor\_pole$  is the number of rotor pole  
 $\theta$  is the rotor position

This function will produce four cycles of sinusoidal waveform during the angular period of the motor behaviour i.e. within  $0^\circ$ - $60^\circ$  with a magnitude between 0-1.

In order to produce a constant overall torque, the contour function for each phase of the motor is non-zero only during its positive inductance slope. Therefore, the choice of the torque contour function for each phase of the SRM is

$$f_T(\theta) = \begin{cases} 0.5 - 0.5 \sin(4.N\_rotor\_pole.\theta) & \theta_1 \leq \theta < \theta_2 \\ = 1 & \theta_2 \leq \theta < \theta_3 \\ = 0.5 + 0.5 \sin(4.N\_rotor\_pole.\theta) & \theta_3 \leq \theta < \theta_4 \\ = 0 & \text{otherwise} \end{cases} \quad (9)$$

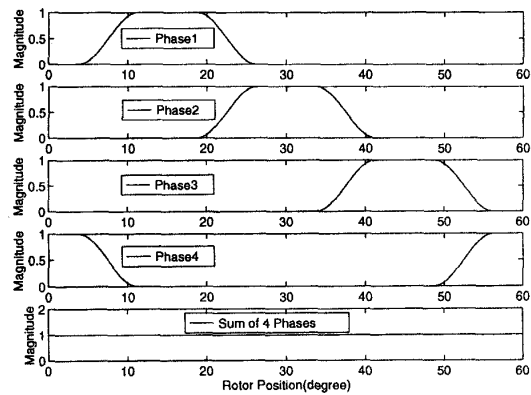


Figure 2 : Torque contour waveform for 4 phases of the SRM

The torque contour waveform for the four phases of the SRM for the torque ripple minimisation technique described in this paper is shown in Figure 2. The sum of the four phase torque contour is unity. In order to obtain the desire torque, the torque contour function is multiply by the desire torque value.

Each of the phase torque contour waveforms is applied to the phase current estimation neural network  $i = h(\hat{T}, \theta)$ . With the information of the rotor position, this neural network is able to generate the required current based on the torque contour waveform. Figure 3 and Figure 4 show how the three neural networks are connected to form the complete system.

IV. SIMULATION AND RESULTS

The training data for all three neural networks were generated by running the motor from standstill to 75rad/s in a normal speed servo simulation. When the motor reached the steady state at 75rad/s, the speed was increased to 150rad/s and subsequently, the speed was reduced to 75rad/s. A total of 100,000 data points were

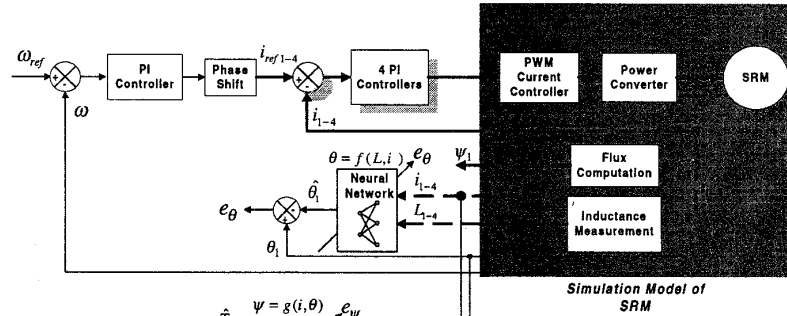


Figure 3 : Data collection and neural networks training

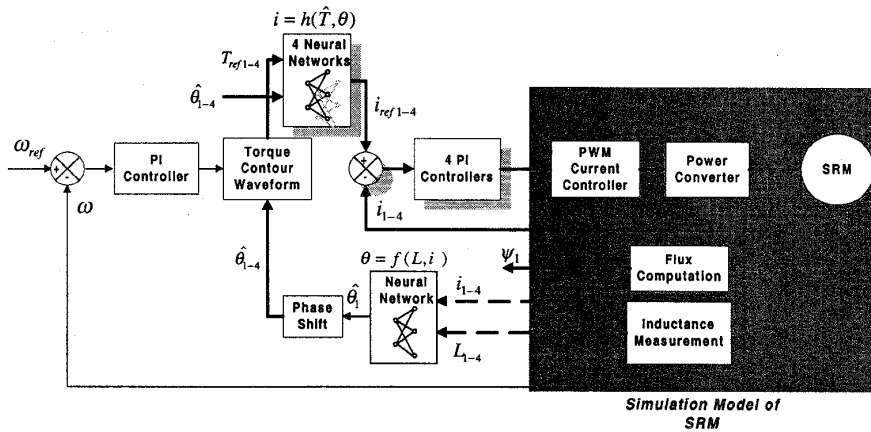


Figure 4: Sensorless control of the SRM

collected for each parameter namely, the angular position  $\theta$ , the phase inductance  $L$ , the phase current,  $i$  phase flux-linkage,  $\psi$  for a simulation time of 10 seconds with a small sample time of 0.1ms. The small sample time was necessary for the simulation to generate an accurate result. The training points were obtained by decimating the original data points by a factor of 5 and thus reducing the training points to 20,000. This reduced the training time significantly compared to training with 100,000 data points.

**1. Rotor Position Estimation**

A two-hidden-layer neural network with five neurons on each hidden layer was trained to approximate the mapping of function  $\theta=f(L,i)$ . The hyper-tangent sigmoid activation function was chosen for the two hidden layers and the linear activation function was used at output layer. After a training time of approximately 2 hours, the neural network has successfully approximated the mapping of  $\theta=f(L,i)$  with a sum squared error of 0.995.

The neural network was validated for an increasing speed of 0-50 rad/s as shown in Figure 5. The neural network has successfully modelled the required function.

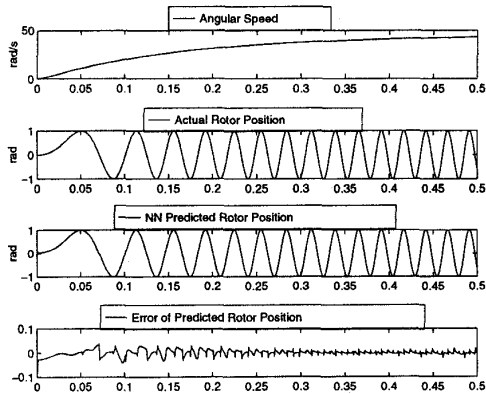


Figure 5 : Neural network rotor position estimation (sine of angular position)

**2. Phase Flux-Linkage And Torque Estimation**

A single hidden layer neural network with five hidden neurons is used to estimate the phase flux-linkage function  $\psi= g(i, \theta)$ .

After a training time of approximately 45 minutes, the neural network has managed to approximate the phase flux-linkage function with a sum squared error of 0.001.

The neural network was validated for an increasing speed of 0-50 rad/s as shown in Figure 6. The neural network has successfully modelled the required function. The estimated torque was computed with equation (7) and a mean square error of 0.79 generated as shown in Figure 7.

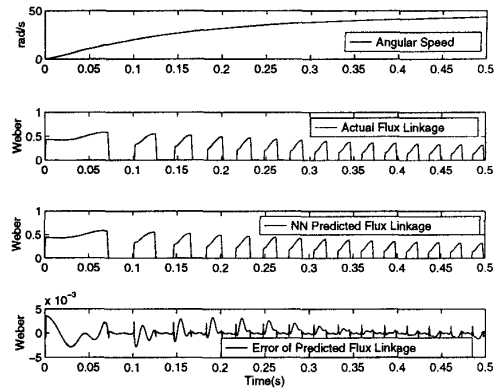


Figure 6: Neural network flux-linkage estimation

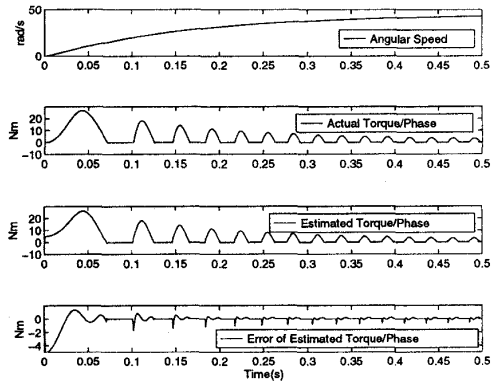


Figure 7: Estimated torque from flux-linkage neural network parameters

**3. Phase Current Estimation**

A two hidden layer neural network with seven neurons on each hidden layer is chosen to approximate the non-linear function of  $i= h(\hat{T}, \theta)$ . After a training time of approximately 1 hour with the Levenberg Marquardt algorithm, the neural network has successfully to approximate the required function with a sum squared error of 2.05.

The neural network was validated for an increasing speed of 0-50 rad/s as shown in Figure 8. The neural network has successfully modelled the non-linear function of  $i= h(\hat{T}, \theta)$ .

#### 4. Torque Ripple Minimisation

The result of the torque ripple minimisation is shown in Figure 9 for an increasing speed of 0-40 rad/s. The maximum torque reference was set to 20Nm. Therefore, within the acceleration period the torque demanded by the SRM was maintained at this value.

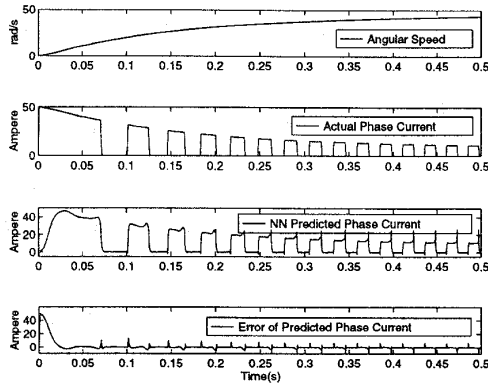


Figure 8: Neural network phase current estimation

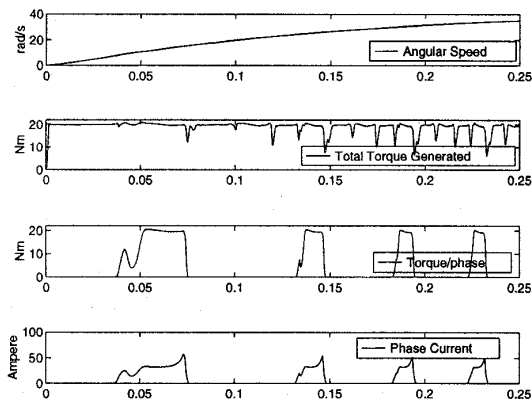


Figure 9: Actual motor torque value at 20Nm and actual phase current

#### V. DISCUSSION

The torque ripple observed at Figure 9 is largely contributed by the error generated in the prediction of the rotor position. Within each interval of the electrical cycle of the rotor position i.e.  $0^{\circ}$ - $60^{\circ}$  of mechanical degree, there are three significant errors which occurred at the unaligned, aligned and the mid point between the two. This is shown in Figure 10. Even though the rotor position neural network was trained to a small sum square of 0.995, this error occurred because the network was not trained with a wide enough set of training data.

In general, the neural networks were able to approximate the non-linear functions of rotor position, flux-linkage and phase current. The neural networks chosen in this simulation have relatively small number of hidden neurons with the maximum number being seven in the phase current estimation neural network. This will allow a fast recall time to be achieved when the sensorless control system is implemented in practical.

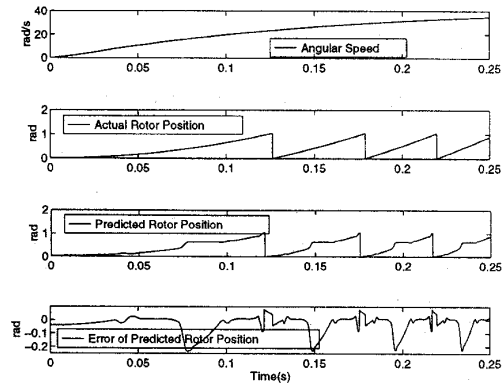


Figure 10: Error in rotor position prediction

#### VI. CONCLUSION

The proposed sensorless control system has shown that torque ripple minimisation can be achieved without a rotor position sensor. In simulation it was shown that it is important to achieve good position prediction accuracy before attempting torque ripple minimisation. A proper training data pattern should be chosen for the neural network during its training phase in order to achieve the generality of the non-linear functions of the SRM.

#### VII. REFERENCE

1. D.S.Reay, T.C.Green, B.W.Williams, 1993, "Application of Associative Memory Neural Networks to the Control of a SRM", *Proc. IECON '93 Int. Conf.*
2. J.G.O'Donovan, P.J.Roche, R.C.Kavanagh, M.G.Egan, J.M.D.Murphy, 1994, "Neural Network Based Torque Ripple Minimisation in a SRM", *IECON '94*
3. D.S.Schramn, B.W.Williams, T.C.Green, 1992, "Torque Ripple Reduction of SRM by Phase Current Optimal Profiling", *IEEE PESC Conf. Rec. '92*
4. I.Hussian, M.Ehsani, 1996, "Torque Ripple Minimization in SRM Drives by PWM Current Control", *IEEE Transactions on Power Electronics*